Proceedings in Manufacturing Systems, Volume 11, Issue 3, 2016, 113–118 ISSN 2067-9238

THE INTERFERENCE AT THE ASSEMBLAGE OF CYLINDRICAL WORM-STAR WHEEL GEAR

Gabriel FRUMUŞANU[1,*], Virgil TEODOR[2], Sofia TOTOLICI[3], Nicolae OANCEA[4]

[1), 4)] Prof., PhD, Manufacturing Engineering Department, "Dunărea de Jos" University of Galaţi, Romania
[2)] Assoc. Prof., PhD, Manufacturing Engineering Department, "Dunărea de Jos" University of Galaţi, Romania
[3)] Assoc. Prof., PhD, Businesses Management Department, "Dunărea de Jos" University of Galaţi, Romania

Abstract: *The cylindrical worm – star wheel gear can be met in practice, for example, in transmissions with kinematical purpose, or in the construction of single screw compressors. Despite having a limited applicability, it presents an important advantage, consisting in the simplicity of its manufacturing. The paper suggests an analytical solution for finding the interference at the assemblage of cylindrical worm – star wheel gear, which is an important matter concerning the design of this type of transmission. The solution lies on a complementary theorem regarding surfaces enveloping, namely the theorem of plain generating trajectories family. An analytical algorithm has been developed in MatLab, in order to implement this solution. A numerical application, which was solved in a concrete case, is also presented.*

Key words: *cylindrical worm – star wheel gear, assemblage, interference, plain generating trajectories family, MatLab.*

1. INTRODUCTION

The cylindrical worm – star wheel gear can be met in practice, for example, in transmissions with kinematical purpose, or in the construction of single screw compressors, Fig. 1.

The study of a gear whose elements have a non-involute profile, in our case the gear formed by a star wheel and its conjugated cylindrical worm, can be realized on the base of the fundamental theorems of the enwrapped surfaces (Olivier, Gohman [2, 3]). It is also possible to solve the same problem by applying complementary theorems – the minimum distance method or the family of substitutive circles theorem [4].

Fig. 1. Single screw compressor [1].

[*] Corresponding author: Domnească str. 111, 800201, Galaţi, Romania;
Tel.: 0236/130208;
Fax: 0236/314463;
E-mail addresses: *gabriel.frumusanu@ugal.ro* (G. Frumuşanu), *virgil.teodor@ugal.ro* (V. Teodor), *sofia.totolici@ugal.ro* (S. Totolici), *nicolae.oancea@ugal.ro* (N. Oancea).

The enhancement of the capacities offered by the graphical design environments (e.g. CATIA) has enabled a new manner to address the particular problems of enwrapped surfaces. It consists in their 3-D modeling, followed by the application of specific algorithms, developed with the help of the dedicated theorems [5].

In this paper, we present an analytical algorithm, developed on the base of the theorem of plain generating trajectories family [6]. This algorithm is a tool for studying the interference that inevitably occurs when the width of star wheel teeth is significant. The method works by following the trajectories drawn by the points from the tooth profile, during the motion involved by the rolling process between the conjugated centrodes associated to the gear elements. The centrode of the worm axial section is rectilinear, while the one of the star wheel is a circle (see Fig. 2).

The next section is dedicated to describe the profile of the star wheel tooth, and to introduce several reference systems, needed to solve the addressed problem. The third section purpose is to find the helical surface of the cylindrical worm flanks, conjugated to the surface of star wheel tooth, as a cloud of points. The fourth section deals with a numerical application of the algorithm, in a concrete case, while the last one is for conclusion.

2. THE STAR WHEEL PROFILE. REFERENCE SYSTEMS

In Fig. 2, there are presented the rolling centrodes associated to the considered enwrapped entities, namely:

- C_1, which is the star wheel centrode – circle of R_e radius (R_e meaning the exterior radius of the star wheel), and
- C_2 – the rectilinear centrode of the conjugated cylindrical worm's axial section.

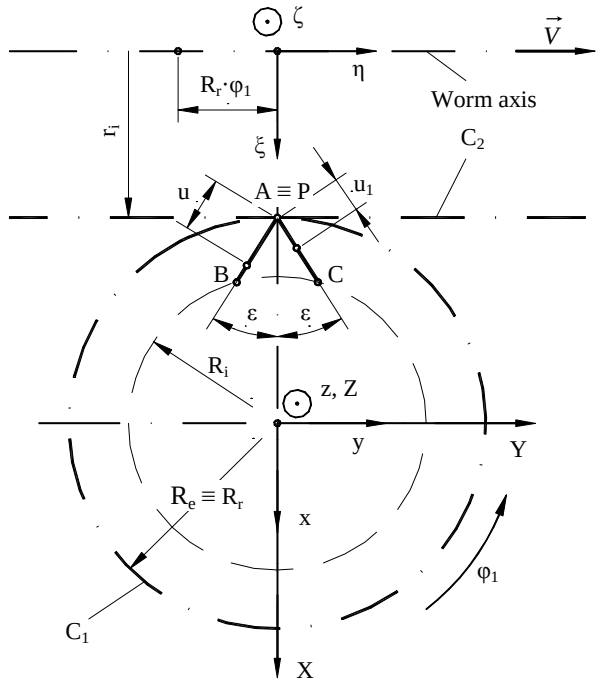

Fig. 2. The rolling centrodes and the reference systems.

The following reference systems are introduced, according to notations from Fig. 2:

- *xyz*, meaning a global system, having *z* – axis overlaid to star wheel rotation axis,
- *XYZ* – relative system, attached to C_1, the star wheel centrode, and
- ξηζ – relative system, attached to C_2, the centrode of worm axial section.

The angular parameter of the star wheel rotation is denoted by φ_1.

If we consider a triangular profile of the star wheel tooth, than the equations of its flanks, $\overline{AB}$ and $\overline{AC}$ are, in *XYZ* reference system:

$$\overline{AB}\left|\begin{array}{l} X=-R_r+u\cdot\cos\varepsilon;\\ Y=-u\cdot\sin\varepsilon;\\ Z=0,\end{array}\right. \tag{1}$$

and

$$\overline{AC}\left|\begin{array}{l} X=-R_r+u_1\cdot\cos\varepsilon;\\ Y=u_1\cdot\sin\varepsilon;\\ Z=0,\end{array}\right. \tag{2}$$

In relations (1) and (2), R_r means the rolling radius (chosen in this case as equal to the exterior radius R_e), while u and u_1 are variable parameters. Their inferior limit value is obviously zero, while the superior limit can be found by imposing to *B* point the condition to belong to the circle of R_i radius:

$$\left(-R_r+u_{\max}\cdot\cos\varepsilon\right)^2+{u_{\max}}^2\cdot\sin^2\varepsilon=R_i^2, \tag{3}$$

and similarly to *C* point (for finding $u_{1\max}$).

3. THE CYLINDRICAL WORM PROFILE

The profile of the cylindrical worm reciprocal enwrapped to the star wheel with triangular tooth profile can be determined by applying diverse methods. Here we present the plain generating trajectories method [6], which supposes the steps from below.

3.1. The relative kinematics

The absolute motions during the gearing process are:

- The star wheel rotation, together with its centrode C_1,

$$x=\omega_3^{\,T}(\varphi_1)\cdot X\ ; \tag{4}$$

- The translation of worm axial section, in correlation with C_1 rotation,

$$\xi=x-a\ ,\ \text{with}\ a=\begin{pmatrix}-(R_r+r_i)\\ -R_r\cdot\varphi_1\\ 0\end{pmatrix}. \tag{5}$$

The equation of the relative motion between the wheel and the worm results from relations (4) and (5):

$$\xi=\omega_3^{\,T}(\varphi_1)\cdot X-\begin{pmatrix}-(R_r+r_i)\\ -R_r\cdot\varphi_1\\ 0\end{pmatrix}. \tag{6}$$

This relative motion determines the families of flanks $(\Sigma_{AB})_{\varphi 1}$ and $(\Sigma_{AC})_{\varphi 1}$ in ξηζ reference system. After replacing the known form of the rotation transform matrix, ω_3 and by developing the equation (6) we obtain:

$$(\Sigma_{AB})_{\varphi 1}\left|\begin{array}{l} \xi=(-R_r+u\cdot\cos\varepsilon)\cos\varphi_1+\\ \qquad +u\cdot\sin\varepsilon\cdot\sin\varphi_1+(R_r+r_i);\\ \eta=(-R_r+u\cdot\cos\varepsilon)\sin\varphi_1+\\ \qquad +u\cdot\sin\varepsilon\cdot\cos\varphi_1+R_r\cdot\varphi_1;\\ \zeta=0,\end{array}\right. \tag{7}$$

for the family of left tooth flanks, and a similar form for the family of right tooth flanks.

3.2. The enveloping condition

We further address to the case of the worm flank reciprocal enwrapped to left tooth flank, the case of the other flank being very similar to the first one. The envelop of $(\Sigma_{AB})_{\varphi 1}$ profiles family is intended to be found by the plane generating trajectories method [6]. In this purpose, the directional parameters of the normal to $\overline{AB}$ profile must be found:

$$\vec{N}_{\Sigma_{AB}}=\begin{vmatrix}\vec{i} & \vec{j} & \vec{k}\\ \cos\varepsilon & -\sin\varepsilon & 0\\ 0 & 0 & 1\end{vmatrix}=-\sin\varepsilon\cdot\vec{i}-\cos\varepsilon\cdot\vec{j}. \tag{8}$$

Hereby, the equations of the normal to $\overline{AB}$ profile result, written in *XYZ* reference system:

$$\vec{N}_{\Sigma_{AB}} \begin{vmatrix} X = -R_r + u \cdot \cos\varepsilon - \lambda \cdot \sin\varepsilon; \\ Y = -u \cdot \sin\varepsilon - \lambda \cdot \cos\varepsilon; \\ Z = 0. \end{vmatrix} \quad (9)$$

The equations of normals trajectories family can now be determined, by using (9) and (6):

$$\left(T_{N_\Sigma}\right)_{\varphi_1} \begin{vmatrix} \xi = \left(-R_r + u \cdot \cos\varepsilon - \lambda \cdot \sin\varepsilon\right)\cos\varphi_1 - \\ \quad -\left(-u \cdot \sin\varepsilon - \lambda \cdot \cos\varepsilon\right)\sin\varphi_1 + R_r + r_i; \\ \eta = \left(-R_r + u \cdot \cos\varepsilon - \lambda \cdot \sin\varepsilon\right)\sin\varphi_1 + \\ \quad +\left(-u \cdot \sin\varepsilon - \lambda \cdot \cos\varepsilon\right)\cos\varphi_1 + R_r \cdot \varphi_1; \\ \zeta = 0. \end{vmatrix} \quad (10)$$

By imposing the condition that the trajectory of a line normal to star wheel tooth flank passes by the gear pole *P* (see Fig. 1),

$$P \begin{vmatrix} \xi_P = r_i; \\ \eta_P = R_r \cdot \varphi_1; \\ \zeta_P = 0, \end{vmatrix} \quad (11)$$

the specific enveloping condition results:

$$\cos\left(\varepsilon - \varphi_1\right) = \frac{R_r \cdot \cos\varepsilon - u}{R_r}. \quad (12)$$

3.3. The worm axial profile

The ensemble formed by equations (7) and (12) determines the axial profile of the worm (the rack-gear) reciprocal enwrapped to the star wheel with triangular tooth profile, having in principle the form:

$$S_{AB} \begin{vmatrix} \xi = \xi(\varphi_1); \\ \eta = \eta(\varphi_1); \\ \zeta = 0. \end{vmatrix} \quad (13)$$

At the same time, a discrete numerical form of the rack-gear profile can be determined:

$$S_{AB} \begin{pmatrix} \xi_1 & \eta_1 & \zeta_1 \\ \xi_2 & \eta_2 & \zeta_2 \\ \cdots & \cdots & \cdots \\ \xi_n & \eta_n & \zeta_n \end{pmatrix}. \quad (14)$$

By giving a helical motion of $\vec{V}$ axis and *p* helical parameter to the vector (14):

$$\begin{pmatrix} \xi_i \\ \eta_i \\ \zeta_i \end{pmatrix}_{i=1\ldots n} = \omega_2{}^T(v) \cdot S_{AB}{}^T - p \cdot v \cdot \vec{j}, \quad (15)$$

an ordinate cloud of points will result, as discrete expression of worm helical flank. Here, *v* means an arbitrary angular parameter, measured for the rotation around $\vec{V}$ axis. If *v* variation interval is discretized in *m* successive points, then the cloud of points describing the helical surface will consist in $m \times n$ points.

3.4. The interference at the assemblage

Because the star wheel tooth flank is, in general, a cylindrical surface with the generatrice perpendicular to worm axis, an interference phenomenon occurs obviously if the two elements (star wheel and worm) are put together in order to form a gear.

The interference can be studied by searching for the intersection point between the worm helical surface and the tooth flank in planes

$$z = H, \quad (16)$$

while *H* parameter take values between zero and half of the star wheel thickness, *B*/2.

The intersection point can be effectively found by numerical calculus. The $\overline{AB}$ segment is firstly discretized in a given number of points having their co-ordinates expressed in ξηζ reference system:

$$\begin{vmatrix} \xi_k = r_i + u_k \cdot \cos\varepsilon; \\ \eta_k = -u_k \cdot \sin\varepsilon; \\ \zeta_k = 0, \end{vmatrix} \quad (17)$$

with $u_k \in [0, u_{\max}]$, $k = 1, 2, \ldots p$.

Then, for each couple (ξ_k, η_k) we have to search for the points belonging to the cloud describing the helical surface, which concomitantly satisfy the condition:

$$\sqrt{\left(\xi_i - \xi_k\right)^2 + \left(\eta_i - \eta_k\right)^2} < eps, \quad (18)$$

and the restriction

$$\left|\zeta_i\right| \le B/2. \quad (19)$$

In relation (18), *eps* means a parameter with a very small, positive value (e.g. 10^{-3}), adopted depending on the intended precision of the calculus.

Hereby, each point (ξ_i, η_i, ζ_i) can be considered as a very close approximation (depending, obviously, on the value being set for *eps* parameter) of the point where the two surfaces (worm / wheel tooth) do intersect in the plane $z = \zeta_i$.

4. NUMERICAL APPLICATION

A numerical application has been developed with the purpose of studying the interference phenomenon. The application approaches the case of a right hand worm, having a single thread and a star wheel with triangular tooth profile.

The nominal values of the parameters defining the geometry of the addressed gear are the following:

- wheel internal radius: R_i = 40 mm;
- wheel external radius: $R_e = R_r$ = 45 mm;
- wheel width: B = 20 mm;
- angle of wheel tooth flank: ε = 30º;
- worm internal radius: r_i = 30 mm;
- worm helical parameter: $p = 5/\pi$ mm.

Table 1

Worm axial profile (co-ordinates)

Crt no.	Left flank		Right flank	
	ξ [mm]	η [mm]	ξ [mm]	η [mm]
1	30.0000	0.0000	30.0000	0.0000
2	30.0051	−0.0029	30.0051	0.0029
3	30.0102	−0.0059	30.0102	0.0059
4	30.0153	−0.0089	30.0153	0.0089
5	30.0205	−0.0118	30.0205	0.0118
6	30.0256	−0.0148	30.0256	0.0148
7	30.0307	−0.0178	30.0307	0.0178
8	30.0358	−0.0207	30.0358	0.0207
9	30.0410	−0.0238	30.0410	0.0238
10	30.0461	−0.0267	30.0461	0.0267
. . . . .				
496	32.6551	−1.7620	32.6551	1.7620
497	32.6606	−1.7661	32.6606	1.7661
498	32.6661	−1.7702	32.6661	1.7702
499	32.6716	−1.7743	32.6716	1.7743
500	32.6771	−1.7785	32.6771	1.7785
501	32.6826	−1.7826	32.6826	1.7826
502	32.6882	−1.7867	32.6882	1.7867
503	32.6937	−1.7909	32.6937	1.7909
504	32.6992	−1.7950	32.6992	1.7950
505	32.7047	−1.7992	32.7047	1.7992
. . . . .				
991	35.3869	−4.0365	35.3869	4.0365
992	35.3923	−4.0415	35.3923	4.0415
993	35.3978	−4.0466	35.3978	4.0466
994	35.4033	−4.0516	35.4033	4.0516
995	35.4088	−4.0567	35.4088	4.0567
996	35.4143	−4.0617	35.4143	4.0617
997	35.4198	−4.0668	35.4198	4.0668
998	35.4252	−4.0718	35.4252	4.0718
999	35.4307	−4.0769	35.4307	4.0769
1000	35.4362	−4.0819	35.4362	4.0819

A dedicated MatLab application has been written in order to implement the algorithm from above for studying the interference. The main steps of the application are the following:

- The superior limit of u parameter, u_{max}, is determined after numerically solving the equation (3), by applying the General method [7].
- The discretization points of $\overline{AB}$ segment are generated, according to (17).
- The worm tooth flank, reciprocal enwrapped to star wheel tooth is determined in discrete form (14) with the ensemble of equations (7) and (12).
- The cloud of points describing the worm helical flank is built by applying to the vector (14) the motion (15).
- All points from the cloud are checked for satisfying the condition (18), with the restriction (19), for each discretization point of $\overline{AB}$ segment; once such a point is found, its co-ordinates are recorded in the solution vector ($\xi_{int\,j}$, $\eta_{int\,j}$, $\zeta_{int\,j}$), j = 1, 2, ...
- The results are exported in numerical form (the solution vector), together to a graphical 3-D representation of the curve formed by the intersection points.

The values of the other parameters involved in solving the addressed numerical application are:

- Number of points for discretizing the tooth flank profile: n = 1000.
- The maximum value of u parameter, calculated by numerically solving (3): u_{max} = 5.8992 mm.
- The interval of variation for v angular parameter (see relation (15)): $v \in [-\pi/20, 0]$.
- Number of points for discretizing the value of v parameter: m = 1000.
- The maximum admissible error to be considered for relation (18): $eps = 5 \cdot 10^{-3}$.

The results obtained after running the MatLab application are below presented in Tables 1, 2 and in Figs. 3–5. Table 1 includes samples of the co-ordinates for the points that give the worm flank profile, in axial section. This profile is depicted, together with the star wheel tooth profile, in Fig. 3.

The co-ordinates of the intersection points between the helical surface of the worm flank and the cylindrical surface of the star wheel tooth flank (the interference points) are sampled in Table 2 – only left flanks case. Fig. 4 presents the 3-D curve obtained by joining the interference points.

In Fig. 5 one can see the part of the star wheel tooth flank being affected by the interference phenomenon, in the left flank case also.

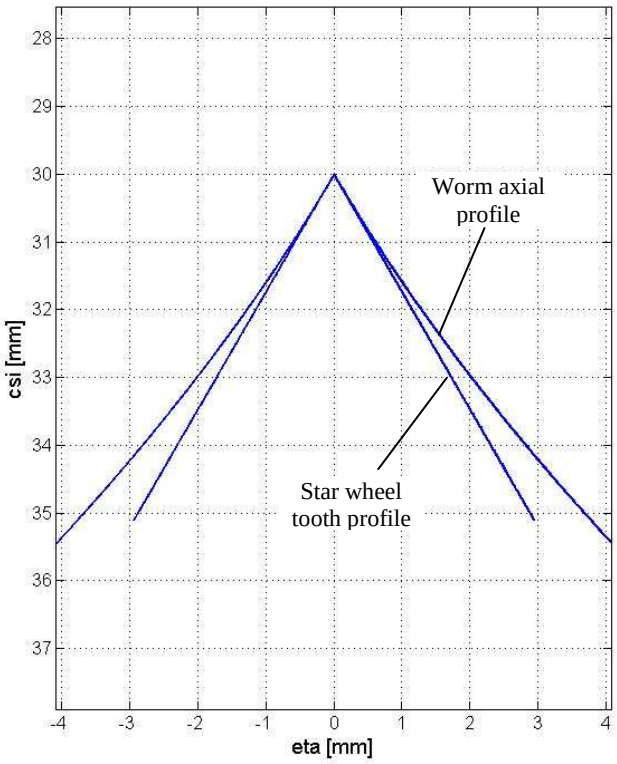

Fig. 3. The reciprocal enwrapped profiles: worm axial profile versus star wheel tooth profile.

Table 2

Interference points (co-ordinates)

Crt. no.	ξ_i [mm]	η_i [mm]	ζ_i [mm]
1	30.4873	−0.2759	4.8287
2	30.4881	−0.2762	4.8239
3	30.4941	−0.2798	4.8200
4	30.5053	−0.2868	4.8168
5	30.5114	−0.2905	4.8128
6	30.5121	−0.2907	4.8080
7	30.5076	−0.2876	4.8024
8	30.5084	−0.2878	4.7976
9	30.5144	−0.2915	4.7937
10	30.5204	−0.2951	4.7897
.....			
486	31.2904	−0.7398	2.5344
487	31.2854	−0.7364	2.5290
488	31.2858	−0.7367	2.5241
489	31.2862	−0.7369	2.5192
490	31.2866	−0.7372	2.5143
491	31.2870	−0.7374	2.5094
492	31.2928	−0.7413	2.5049
493	31.2986	−0.7452	2.5004
494	31.2990	−0.7454	2.4955
495	31.2940	−0.7420	2.4901
.....			
971	30.2210	−0.1222	0.0424
972	30.2055	−0.1132	0.0377
973	30.1900	−0.1043	0.0330
974	30.1796	−0.0985	0.0283
975	30.1590	−0.0865	0.0236
976	30.1436	−0.0777	0.0189
977	30.1230	−0.0659	0.0141
978	30.1024	−0.0541	0.0094
979	30.0716	−0.0363	0.0047
980	30.0152	−0.0039	0.0000

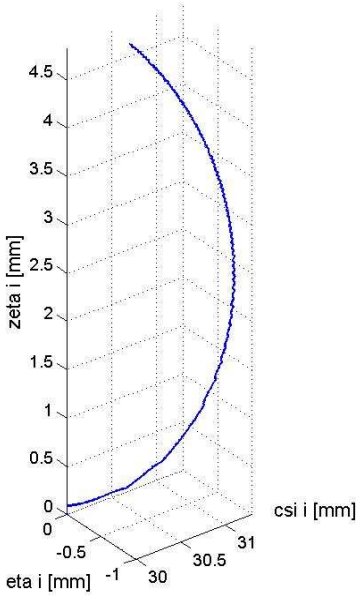

Fig. 4. The interference point's locus.

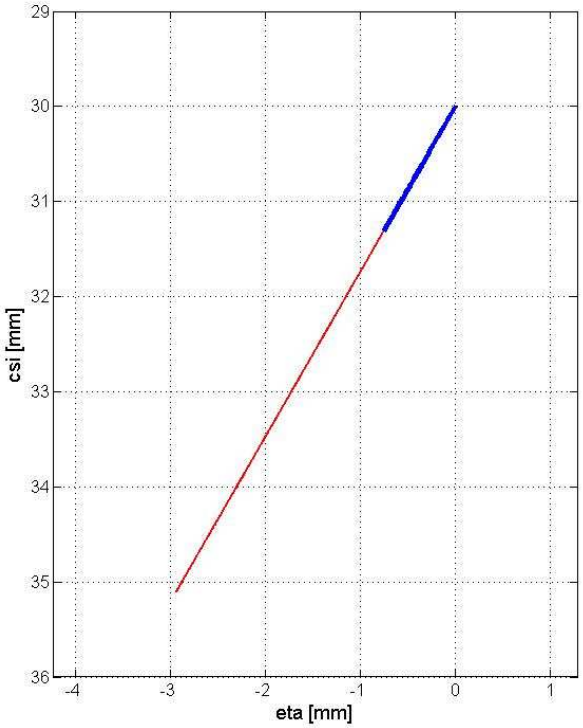

Fig. 5. The zone of the tooth flank affected by interference, referred to the entire flank length.

In Fig. 5 the zone of the flank affected by interference is represented thicker. By refering it to entire tooth flank length, it represents about 24.88 %.

By using the same Matlab application, we further present an analysis of the impact brought by gear elements geometry and dimensions onto the importance of the interference phenomenon.

In the mentioned purpose, the following parameters have been successively modified, one at a time (the rest of them remaining at their standard values), and the effect onto the interference has been assessed:

- Angle of wheel tooth flank: $\varepsilon = 20^o, 30^o, 40^o$.
- Worm internal radius: $r_i = 20, 30, 40$ mm.
- Worm helical parameter: $p = 5/\pi, 7/\pi, 9/\pi$ mm.

The effect of modifying the tooth flank angle can be noticed in Fig. 6. When $\varepsilon = 20^o$, the fraction of the flank length affected by interference increases to 29.91 %, while for $\varepsilon = 40^o$, the same fraction diminishes to 19.21 % (see also Fig. 7,*a*).

The effect of worm internal radius variation is presented in Fig. 7,*b*. For $r_i = 20$ mm, the fraction of the flank length affected by interference is about 30.49 %, and for $r_i = 40$ mm, the corresponding fraction is smaller – 21.96 %.

The effect of changing the worm helical parameter can be observed in Fig. 7,*c*. If $p = 5/\pi$ mm, then the fraction of the flank length affected by interference is about 35.1 %, while if $p = 7/\pi$ mm, then the fraction increase even more, to 44.31 %.

For concluding this analysis, we can state that the values of the specific parameters, adopted at the design stage for the gear formed by a star wheel and a cylindrical worm, have a major impact from the interference phenomenon point of view.

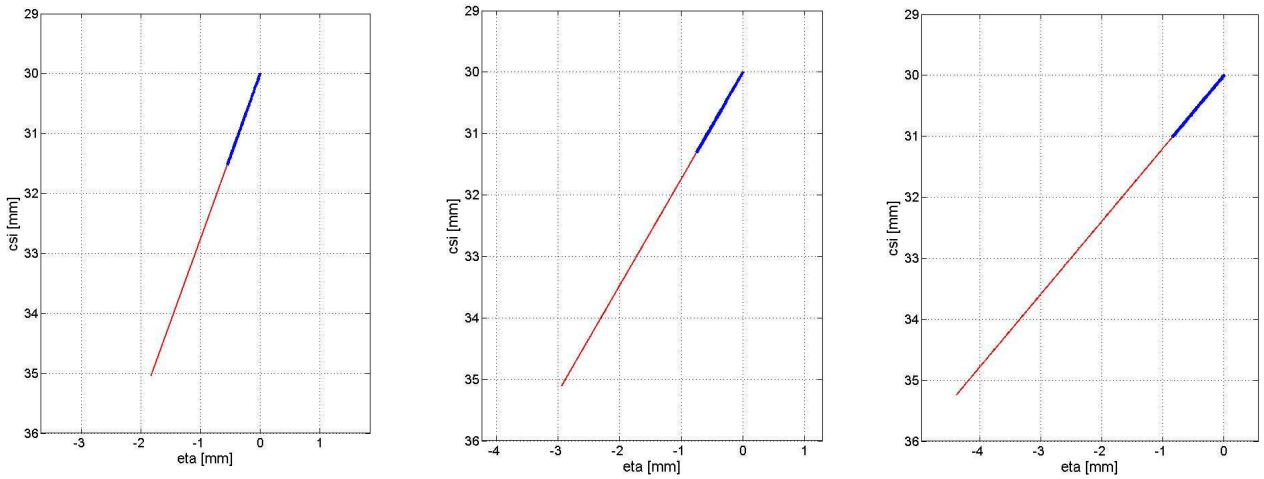

a b c

Fig. 6. The impact of the tooth flank angle onto the interference phenomenon extension: *a* – ε = 20º, *b* – ε = 30º, *c* – ε = 40º.

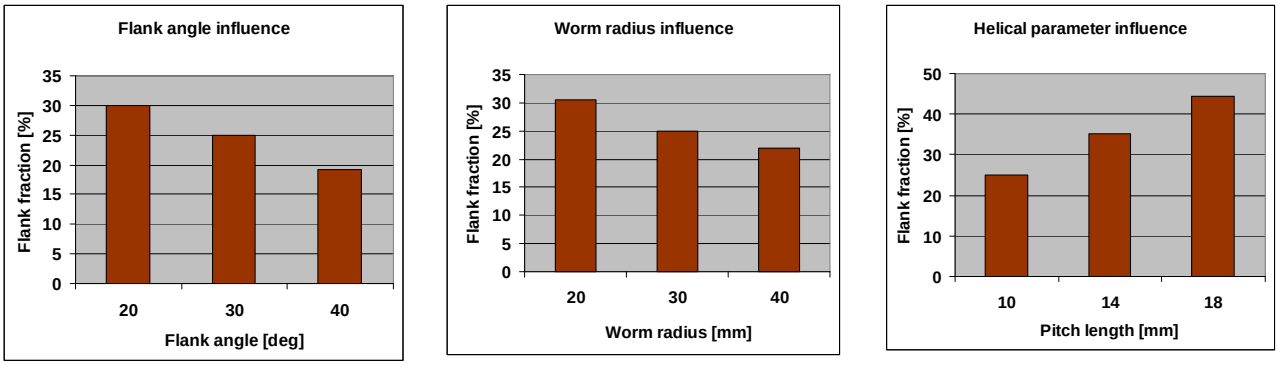

a b c

Fig. 7. The dimension of the interference phenomenon depending on: *a* – Flank angle, *b* – Worm radius, *c* – Helical parameter.

5. CONCLUSIONS

This paper presents a solution to study the interference at the assemblage of the cylindrical worm - star wheel gear. The solution lies on the theorem of the plane generating trajectories family and enables to find both the worm axial profile, reciprocal enwrapped to the star wheel tooth profile, and the points of intersection between the two profiles, in planes normal to star wheel axis. The numerical implementation of the method in a concrete case has enabled us to prove the method feasibility.

The analysis of the dependence between the constructive parameters of the addressed gear and the magnitude of the interference phenomenon has shown an important potential to improve the gear functioning if properly designed. Hereby, beyond the obvious solution of reducing the star wheel thickness, a smaller tooth flank angle, and a higher diameter of the worm combined with a smaller value of the worm helical parameter lead to a significant diminishing of the interference occurrence.

Here, a triangular profile of the star wheel tooth has been considered, but other profile shapes should be further developed in order to improve even more this type of transmission.

ACKNOWLEDGEMENTS: This work was supported by a grant of the Romanian National Authority for Scientific Research and Innovation, CNCS – UEFISCDI, project number PN-II-RU-TE-214-4-0031.

REFERENCES

[1] *Compressor Airend & Rebuilts*, available at `http://www.nirvatech.com/products.php?pageID=9&catID=29&productID=27`
[2] F.L. Litvin, *Theory of gearing*, NASA, Scientific and Technical information Division, Washington DC, 1984.
[3] S.P. Radzevich, *Kinematics Geometry of Surface Machining*, CRC Press, London, 2008.
[4] N. Oancea, *Surfaces generation through winding, vol. I – III*, Galati University Press, Galaţi, 2004.
[5] N. Baroiu, V. Teodor, N. Oancea, *A new form of in plane trajectories theorem. Generation with rotary cutters*, Bulletin of the Polytechnic Institute of Iaşi, Tome LXI (LV), Fasc. 3, 2015, pp. 29–36.
[6] V. Teodor, *Contributions to the elaboration of a method for profiling tools – Tools which generate by enwrapping*, Lambert Academic Publishing, Saarbrucken, 2010.
[7] G. Frumuşanu, *Metode numerice în ingineria tehnologică*, Edit. Cartea universitară, Bucharest, 2004.